



## Tracing winter temperatures over the last two millennia using a NE Atlantic coastal record

5 Irina Polovodova Asteman<sup>1</sup>, Helena L. Filipsson<sup>2</sup>, Kjell Nordberg<sup>1</sup>

<sup>1</sup> Department of Marine Sciences, University of Gothenburg, Carl Skottbergsgata 22B, 41319 Gothenburg, Sweden

<sup>2</sup> Department of Geology, University of Lund, Sölvegatan 12, 22362 Lund, Sweden

*Correspondence to:* Kjell Nordberg ([kjell.nordberg@marine.gu.se](mailto:kjell.nordberg@marine.gu.se))



**Abstract.** We present 2500 years of reconstructed winter temperatures by using a fjord sediment archive from the NE Atlantic. The study is based on ca. 8-m long sediment core from Gullmar Fjord (Sweden), dated by  $^{210}\text{Pb}$  and AMS  $^{14}\text{C}$  and analysed for stable oxygen isotopes ( $\delta^{18}\text{O}$ ) measured on shallow infaunal benthic foraminiferal species *Cassidulina laevigata*. The bottom water temperatures (BWTs), calculated by using a palaeotemperature equation of McCorkle et al (1997), range between 2.7 - 7.8°C and are within the annual temperature variability, instrumentally recorded in the deep fjord basin since the 1890s. The record demonstrates a warming during the Roman Warm Period (~350 BCE – 450 CE), variable bottom water temperatures during the Dark Ages (~450 – 850 CE), positive bottom water temperature anomalies during the Viking Age/Medieval Climate Anomaly (~850 – 1350 CE) and a long-term cooling with distinct multidecadal variability during the Little Ice Age (~1350 – 1850 CE). The fjord BWT record also picks up the contemporary warming of the 20<sup>th</sup> century, which does not stand out in the 2500-year perspective and is of the same magnitude as the Roman Warm Period and the Medieval Climate Anomaly.

## 1 Introduction

The climate variability over last two millennia has been widely recognized as crucial for the understanding of the present and future climate responses to anthropogenic forcing (e.g. Cunningham et al., 2013; Pages2k, 2013; McGregor et al., 2015; Abram et al., 2016). To evaluate how significant regional climate changes are or if observed temperature anomalies are unprecedented in view of long-term climate evolution, there is a need for long historical instrumental climate records. A major limiting factor for the reconstructions of past climate changes, both by using proxy data and paleoclimate modelling, is often a lack of such long instrumental records, which if available seldom reach beyond the 20<sup>th</sup> century. The North Atlantic region plays in this respect a paramount role for climate variability by modulating the European climate through e.g. changing intensity of the Atlantic Meridional Overturning Circulation (AMOC) (e.g. Eiríksson et al., 2006; Lund et al., 2006; Park and Latif, 2008; Trouet et al., 2009). Hence, high-resolution paleoceanographic records, which preferably overlap with instrumental observations and historical data, are needed from the North Atlantic. At the same time many marine records available from the region to date naturally tend to have low temporal resolution due to location in the deep-sea or within the open shelf areas. At the same time, crucial knowledge has been gained from temperature proxy datasets available to date from the North Atlantic and northern hemisphere, which represent either composite records of different climate characteristics with various temporal resolution or are a combination of historical and proxy data; with generated data sets mostly reflecting summer conditions in higher latitudes (e.g. Moberg et al. 2005; Gunnarsson et al., 2011; Butler et al., 2013; Cunningham et al., 2013; PAGES2K, 2013, 2017; Sicre et al., 2014; Linderholm et al., 2015). In contrast, based on instrumental records, increased winter temperatures have been suggested as important driver of the most recent warming (Cage and Austin, 2010) and, hence, climate proxies incorporating winter signal are needed. Sediment archives of the fjord inlets located within the North Atlantic region offer the potential of high-resolution records of maritime climate, acting as sediment traps resolving climate variability at nearly annual resolution (Howe et al., 2010). Yet to date, there are relatively



few such high-resolution paleoclimate records from the North Atlantic fjords spanning the late Holocene (among others Mikalsen et al., 2001; Klitgaard-Kristensen et al., 2004; Cage and Austin, 2010; Filipsson and Nordberg, 2010; Hald et al., 2011, Kjennbakken et al., 2011; Faust et al., 2016).

Herein, we present a high-resolution winter temperature proxy record from the Gullmar Fjord, on the west coast of Sweden, which illustrates the climate development in NW Europe over the last ~2500 years. The reconstructed temperatures are based on stable oxygen isotopes ( $\delta^{18}\text{O}$ ) measured in shells (tests) of a shallow infaunal foraminifer *Cassidulina laevigata* and reflect the deep-water temperatures in the fjord basin. The fjord has a >100-yr long record of instrumental observations from the deepest basin, performed since 1869 (Fig. 2A-C); furthermore, >100-yr long time series of air temperature observations are also available for Stockholm, Sweden and central England. These instrumental observations of bottom water - and air temperatures are used to evaluate the accuracy of the reconstructed climate variability for the last century provided by the fjord sediment archive.

## 2 Study area

Gullmar Fjord is a Skagerrak fjord inlet, which is 28 km long and 1-2 km wide and oriented south-west to north-east (Fig. 1). The maximum basin depth is 118.6 m. The fjord is located at critical latitude picking up fluctuations between cold and temperate climates and has almost no tidal activity. The adjacent Skagerrak largely determines the local hydrography so that the deep (basin) water, which is typically exchanged in the fjord during the winter, originates from the North Sea surface water flowing into the Skagerrak with the present-day current circulation system (Svansson, 1975; Nordberg, 1991). The 42-m deep sill at the fjord entrance restricts the water exchange and results in water column stratified due to salinity differences (Fig. 1C). At the surface (<1m) there is a thin layer of river water from the Örekilsälven (Fig. 1), which does not significantly impact the fjord hydrography (SMHI, 1994; Arneborg, 2004). Below at 1-15 m water depth there is a brackish water mass (S=24-27), primarily derived from the brackish Baltic current flowing northward along the Swedish west coast. The brackish water mass has a residence time of 20-38 days in Gullmar Fjord (Arneborg et al., 2004). A more saline water mass (S=32-33) at ~15-50 m is derived from the Skagerrak and has mean residence time of 29-62 days (Arneborg et al., 2004). The last and deepest layer (>50 m), referred herein as deep water or basin water, is more stagnant, with little seasonal and inter-annual changes in salinity ranging between 34 and 35 and inter-annual temperature variability of 4 - 8°C (Fig. 2A, B). The deep water temperatures vary between the years depending on the temperature of the inflowing water mass but remain stable seasonally (Fig. 2D). The deep-water salinities seasonally do not vary much from the average value of 34.5 (Fig. 2B). The stratification of the water column is strengthened during the summer by the development of a strong thermocline. The deep-water exchange of the fjord basin water takes place once a year during winter, mostly between January and March. Due to a presence of a sill and the large basin volume, the temperature and salinity of the inflowing North Sea/Skagerrak water, is preserved in the basin until the next turnover, which often occurs in the following year (Arneborg et al., 2004). The benthic foraminifers reproduce and grow in the fjord during the following spring-summer-autumn (Gustafsson and Nordberg 2001),



incorporating the winter-signal in their shells. This results in a stable oxygen isotope signal mainly reflecting winter temperatures of the North Sea surface water and the Skagerrak intermediate water.

After an extensive deep-water exchange event in the fjord the oxygen level starts to decline in June, and the lowest oxygen levels normally develop between November and January, usually dropping below 2 ml O<sub>2</sub> l<sup>-1</sup> indicating hypoxic conditions, but anoxia has not been recorded (Fig. 2F). The first ever documented severe hypoxic event was noted in February 1890 by Pettersson and Ekman (1891). In the following, severe hypoxic events ( $\leq 1$  ml O<sub>2</sub> l<sup>-1</sup>) were measured in 1906, 1961/62, and 1973/74 (Fig. 2C) but due to the low observation frequency and duration of these events are not well documented. Since 1979, multiple episodes of more frequent severe hypoxia lasting for at least 3 months have been observed. These events occurred in 1979/80, 1983/84, 1987/88, 1988/89, 1990/91, 1994/95, 1996–1998, 2008, 2014/2015 (e.g. Filipsson and Nordberg 2004a; Polovodova Asteman and Nordberg 2013; SMHI SHARK-database, 2017).

The severe hypoxia makes the fjord basin hostile for large burrowing organisms but allows benthic meiofaunas to thrive. This lowers sediment bioturbation and results in well-preserved environmental sediment archive. The fjord basin has high sediment accumulation rates, which provide a high temporal resolution corresponding to 1-6 years per 1-cm thick sediment sample. Finally, the fjord sediment archive is characterized by the diverse and abundant foraminiferal faunas and dinoflagellate cysts, which have already provided some insights in climate evolution and associated environmental changes on the Swedish west coast during the last two millennia (Filipsson & Nordberg, 2004a; Harland et al., 2006; Nordberg et al. 2009; Filipsson and Nordberg 2010; Polovodova et al., 2011; Harland et al., 2013; Polovodova Asteman & Nordberg, 2013; Polovodova Asteman et al., 2013).

### 3 Material and Methods

This study is based on a composite record of two sediment cores: GA113-2Aa and 9004, which were both collected at 116 m water depth in the deepest Gullmar Fjord basin (58°17.570' N, 11°23.060' E) (Fig. 1), for which the long-term hydrographic observations are available (Fig. 2A-C). The core 9004 (731-cm long) was taken with a gravity corer ( $\varnothing=7.6$  cm) aboard of *R/V Svanic* in July 1990. The core GA113-2Aa (60-cm long) with an intact sediment-bottom water interface was recovered by using a Gemini corer ( $\varnothing=8$  cm) in June 1999 from the *R/V Skagerak*. In the laboratory both cores were split in two halves and sectioned in 1-cm intervals. One half was used for bulk sediment geochemistry (TC, TN and C/N ratio), stable oxygen and carbon isotopes, dinoflagellate cysts- and benthic foraminiferal faunal analyses. Another half was stored as an archive at the Department of Geosciences, University of Gothenburg. The TC and stable carbon isotope data from both cores are published in Filipsson and Nordberg (2010), dinoflagellate cysts data are discussed in Harland et al. (2006, 2013), while C/N and foraminiferal assemblage data are presented in Filipsson & Nordberg (2004a), Polovodova et al. (2011) and Polovodova Asteman et al. (2013). We also present data from the gravity core G113-091, collected at the same location as GA113-2Aa & 9004 aboard of *R/V Skagerak* in September 2009, and used herein only (similar to our previous study) to create a composite age model for the cores GA113-2Aa and 9004 (Polovodova Asteman et al., 2013; see below).



In addition to the above-mentioned cores, we also use six surface samples (0-1cm) collected at five stations in the Skagerrak (OS4, OS6, OS14, 9202 and 9205) and one station in the Gullmar Fjord (G113-091a: the same location as for GA113-2Aa & 9004) in 1992-93 and 2009, respectively (Fig.1B, C; Table 1). All surface samples were stained by rose Bengal to distinguish individuals presumably living at the moment of sampling from the empty foraminiferal shells.

### 5 3.1 Sediment core dating and age model

The age model for GA113-2Aa and 9004 has been previously published in Filipsson and Nordberg (2010) with further revisions by Polovodova et al. (2011) and Polovodova Asteman et al. (2013). Eleven intact marine bivalve shells were recovered in life position from the core 9004 and were subject to the AMS  $^{14}\text{C}$  analysis (Fig. 3A; Table 2). All  $^{14}\text{C}$  dates were obtained through analysis at the Ångström Laboratory (Uppsala University, Sweden) and originally were calibrated using the marine calibration curve (Reimer et al., 2004; Bronk Ramsey, 2005). Ages were normalized to  $\delta^{13}\text{C}$  of  $-25\text{‰}$  according to Stuiver and Polach (1977), and a correction corresponding to  $\delta^{13}\text{C} = 0\text{‰}$  (not measured) versus PDB has been applied. Herein we present ages recalibrated by using Calib Radiocarbon Calibration software v. 7.1 (Stuiver et al., 2017; <http://calib.org/calib/>), the most recent marine calibration curve (Reimer et al, 2013) and a reservoir age of 500 yr ( $\Delta R = 100 \pm 50$ ), which has been obtained on pre-bomb marine bivalve shells from the Gullmar Fjord, provided by the Natural History Museums in Gothenburg and Stockholm (Nordberg and Posnert, unpubl. data). All ages are presented as median probability with  $1-\sigma$  error margin (Table 2). Two dates at 98 cm and 313 cm showed minor age reversals and were omitted from the final age model (Table 2). The core GA113-2Aa was dated by using  $^{210}\text{Pb}$  and a constant rate of supply (CRS) model (Appleby and Oldfield, 1978), which suggested that the core material was deposited between ca. 1915 and 1999 (Fig. 3A). For details regarding GA113-2Aa age model see Filipsson and Nordberg (2004a).

Together the cores GA113-2Aa & 9004 proved to be a continuous sediment record with no gap in between based on correlation of the stable carbon isotopes ( $\delta^{13}\text{C}$ ) and benthic foraminiferal species *C. laevigata*, *Adercotryma glomerata* and *Hyalinea balthica* with respective data from the core G113-091 (Fig. 3B herein; Polovodova Asteman et al., 2013; Polovodova Asteman and Nordberg, 2013). The composite record of GA113-2Aa & 9004 spans from approximately 350 BCE to 1999 CE (Table 2, Fig. 3A), and includes the late Holocene climate events such as the Roman Warm Period (RWP: ~350 BCE – 450 CE), the Dark Ages Cold Period (DA: ~450 – 850 CE), the Viking Age/Medieval Climate Anomaly (VA/MCA: ~850 – 1350 CE), the Little Ice Age (LIA: ~1350 – 1850 CE) and the contemporary warming from 1850 CE to present (Lamb, 1995; Filipsson and Nordberg, 2010; Harland et al., 2013; Polovodova Asteman et al., 2013; Helama et al., 2017). We add the Viking Age to the Medieval Climate Anomaly following the approach of Filipsson and Nordberg (2010), based on historical evidence that warming in Northern Europe began earlier than 1000 CE, which allowed Vikings to reach the NE coast of England and loot the monastery of Lindisfarne in 793 CE (Morris, 1985). For further details on chronology of the cores GA113-2Aa and 9004 see Filipsson and Nordberg (2004a), Polovodova et al., 2011; and Polovodova Asteman et al. (2013).



Combining the long gravity core with the 60 cm long Gemini core, which includes the sediment-bottom water interface and, hence, the intact core top, resulted in a high-resolution temporal record of almost 1-year  $\text{cm}^{-1}$  sample for the upper part of the record and  $<10$  years  $\text{cm}^{-1}$  sample for the deepest part of the record. Calculations from the  $^{210}\text{Pb}$  analyses and the AMS- $^{14}\text{C}$  dates suggest sediment accumulation rates of  $\sim 9$  mm  $\text{year}^{-1}$  in the most recent sediments and approximately  $\sim 2.8$  mm  $\text{year}^{-1}$  in the compacted deepest part of the gravity core (Fig. 2). Hence, due to high accumulation rates the upper 60 cm of the record can be directly compared to instrumental hydrographic and meteorological data (Figs 6, 7).

### 3.2 Stable oxygen isotopes

We measured  $\delta^{18}\text{O}$  on tests of shallow infaunal foraminifer *Cassidulina laevigata* from the core top samples and from the ca. 8-m long G113-2Aa - 9004 record (Fig.1B). Between 12 and 20 specimens of *Cassidulina laevigata* were picked from each sample for the analysis. In total 6 and 425 samples were analysed for stable oxygen isotopic composition for the surface sediments and composite G113-2Aa - 9004 record, respectively. All samples were measured at the Department of Geosciences, University of Bremen, Germany, using a Finnigan Mat 251 mass spectrometer equipped with an automatic carbonate preparation device. Isotope composition is given in the usual  $\delta$ -notation and is calibrated to Vienna Pee Dee Belemnite (V-PDB) standard. The analytical standard deviation is  $<0.07\text{‰}$  for  $\delta^{18}\text{O}$  based on the long-term standard deviation of an internal standard (Solnhofen limestone).

The temperature was reconstructed using the salinity:  $\delta^{18}\text{O}_w$  relationship established by Fröhlich et al. (1988) (eq. 1), which is representative for this region (Filipsson, unpubl. data). An average salinity value of 34.4 (range 33-35) was used in equation 1, based on instrumental measurements between 1896 and 1999 for the fjord deep-water (station Alsäck). The salinity ( $S$ ) was assumed to be constant over the investigated time period.

$$\delta^{18}O_w = 0.272 \times S - 8.91 \quad (1)$$

To calculate temperatures the paleotemperature equation by McCorkle et al. (1997) was applied (eq. 2). This equation is more appropriate to the temperature range observed in fjord basin than the more commonly used linear equation by Shackleton (1974), which produces unrealistically high temperatures (see results section). The bottom water temperature in degrees Kelvin ( $T$  °K) was calculated as follows:

$$T^{\circ}K = \sqrt{\frac{2.78 \times 10^3}{\ln\left(\frac{\delta^{18}O_c + 1000}{0.97006 \times \delta^{18}O_w - 29.94} + 1000\right)}} + \frac{2.89}{10^3} \quad (2)$$

Here,  $\delta^{18}O_c$  stands for stable oxygen isotopic ratio  $^{18}\text{O}/^{16}\text{O}$  measured in calcite tests of *C. laevigata*, while  $\delta^{18}O_w$  is the isotopic composition of water calculated from equation 1 and converted from SMOW to V-PDB by subtracting  $0.27\text{‰}$  (Bemis et al., 1998)

30



Finally, to convert reconstructed temperatures to degrees Celsius, equation 3 was used:

$$T^{\circ}\text{C} = T^{\circ}\text{K} - 273.15 \quad (3)$$

- 5 Since 1990 *C. laevigata* has become a rare species in the Gullmar Fjord deep basin (Fig. 6), which resulted in short gap in the most recent part of the record. Similar gaps in  $\delta^{18}\text{O}$  and, hence, bottom water temperature data are also seen for the earlier part of the record and are due to absence or very low abundances of *C. laevigata* (Fig. 6).

### 3.3 Hydrographical and meteorological instrumental data

Long-term hydrographical instrumental data for temperature, salinity and dissolved oxygen concentration [ $\text{O}_2$ ] for the fjord basin (average for 110-118 m w.d.) were extracted from the Swedish Meteorological and Hydrological Institute (SMHI) SHARK database (<https://www.smhi.se/klimatdata/oceanografi/havsmiljodata/marina-miljoovervakningsdata>). Some of the Gullmar instrumental data is also available from the Water Quality Association of the Bohus Coast (BVVF) (<http://www.bvvf.se/>), while the data prior to 1958 come from Engström (1970). The Skagerrak hydrography data for the stations adjacent to OS4-6, 9202, 9205 and OS14 were obtained from the International Council for the Exploration of the Seas (ICES: <http://www.ices.dk/marine-data/>).

Meteorological observations of air temperature were also obtained for Stockholm (<https://www.smhi.se/klimatdata>) and the Central England (<http://www.metoffice.gov.uk/>), which both have the longest historical meteorological records going as far back as the 18<sup>th</sup> century.

## 4 Results

### 4.1 Core tops

To obtain an error estimate and to facilitate the choice of the paleotemperature equation we used stained tests of *Cassidulina laevigata* from the core top samples collected in the Gullmar Fjord and the adjacent Skagerrak. Calculated bottom water temperatures based on the  $\delta^{18}\text{O}_c$  values from the living (stained) *C. laevigata* were compared to ICES and SMHI hydrography data from the adjacent stations (Fig. 4A). Also the  $\delta^{18}\text{O}_c$  values predicted from the chosen equation (see below) were used to estimate the reliability of our temperature reconstruction (Fig. 4B). *Cassidulina laevigata* has been previously suggested to calcify 0.19‰ lower than equilibrium (Poole et al., 1994). Our  $\delta^{18}\text{O}_c$  data from the core tops demonstrate an offset, ranging between 0.01‰ and 0.27‰ (mean 0.15‰), compared with  $\delta^{18}\text{O}_c$  predicted using the palaeotemperature equation from McCorkle et al (1997) (Fig. 4B). Applying the mean correction of +0.15‰ to the Gullmar  $\delta^{18}\text{O}_c$  record results in bottom water temperatures ~0.5-1°C higher than those recorded by instrumental observations in the fjord (Fig. 2A), while uncorrected  $\delta^{18}\text{O}_c$  values produce temperatures close to observations. Taking the latter into the account and because based on



available data it is difficult to estimate how large the correction should be, we further report the uncorrected  $\delta^{18}\text{O}_c$  values both for the core tops and for the sediment cores. Instead, we use a median value ( $0.7^\circ\text{C}$ ) of the range in produced temperature offset (Fig. 4A) as an error margin for our paleotemperature reconstructions (Figs 5-6).

Instrumental temperature data from ICES and SMHI were used to calculate  $\delta^{18}\text{O}_c - \delta^{18}\text{O}_w$  for the core top samples to facilitate the choice of a paleotemperature equation. Plotting  $\delta^{18}\text{O}_c - \delta^{18}\text{O}_w$  versus observed temperature data for different paleotemperature equations (Fig. 4C) allows estimating which of the equations gives the best possible agreement with the core top data and, hence, is the most appropriate for temperature reconstructions. Figure 4C shows that  $\delta^{18}\text{O}$  values from the NW Skagerrak (OS4 and OS6) are clearly in better agreement with equations by Hays and Grossman (1991) and McCorkle et al. (1997), while the central Skagerrak samples (9202 and 9205) plot close to the linear equation by Shackleton (1974). The Gullmar Fjord (G113-091) and the OS14 station, taken just outside the fjord, occupy a space in between the Shackleton equation and those by Hays and Grossman (1991) and McCorkle et al. (1997). This suggests that applying the Shackleton equation for Gullmar Fjord and Skagerrak will result in temperatures higher than observations, which has been also observed for *Cibicidoides* and *Planulina* from Florida Straits (Marchitto et al., 2014). Indeed, when testing the Shackleton equation on our dataset, the temperatures are warmer than the ICES hydrographic observation data by  $1.5\text{--}2^\circ\text{C}$ . In contrast, the equation by Bemis et al. (1998) applied to the core top  $\delta^{18}\text{O}_c$  data produces the coldest temperatures, which are  $0.9\text{--}1.9^\circ\text{C}$  colder than observations. In turn, it appears that by using Hays and Grossman (1991) or McCorkle et al. (1997) equations, the corresponding calculated temperatures come closer to observations. Both equations are nearly identical for the temperature range  $5\text{--}8^\circ\text{C}$  (Fig. 4C) observed between 1890 and 2001 (Fig. 2) and by exercising both equations on Gullmar Fjord  $\delta^{18}\text{O}_c$  record the almost identical paleotemperature curves are produced. This is rather curious because the equation of Hays and Grossman (1991) is based on meteoric calcite of non-biogenic origin. For this reason, in the current paper we apply the McCorkle et al (1997) equation for the paleotemperature reconstructions.

#### 4.2 Composite record of G113-2Aa and 9004 sediment cores

The  $\delta^{18}\text{O}$  record from the Gullmar Fjord shows both decadal and centennial variability for the last 2500 yr (Fig. 5) and can be divided in five major isotopic intervals: 1) For the lower part of the record at 802–592 cm, corresponding to  $\sim 350\text{ BCE} - 450\text{ CE}$ , the  $\delta^{18}\text{O}_c$  values are generally lower ( $\sim 2.4\text{‰}$ ) than the long-term average of  $2.7\text{‰}$ . 2) Between 598 and 475 cm ( $\sim 425 - 900\text{ CE}$ ) the  $\delta^{18}\text{O}$  record demonstrates a considerable variability (Fig. 5), starting with higher  $\delta^{18}\text{O}_c$  ( $2.8\text{--}3\text{‰}$ ) at 598–574 cm ( $\sim 425 - 525\text{ CE}$ ), which then become lower ( $\sim 2.4\text{‰}$ ) at 574–529 cm ( $\sim 525 - 700\text{ CE}$ ) and increase again ( $\sim 3.0\text{‰}$ ) between 529 and 497 cm ( $\sim 700 - 825\text{ CE}$ ). 3) The 475–302 cm interval ( $\sim 900 - 1350\text{ CE}$ ) displays again lower  $\delta^{18}\text{O}_c$  ( $\sim 2.4\text{--}2.5\text{‰}$ ), which are below the long-term average. 4) From 302 to 53.5 cm ( $\sim 1350 - 1900\text{ CE}$ ) the stable oxygen isotope record increases again with the majority of the  $\delta^{18}\text{O}_c$  values being  $\sim 3.1\text{--}3.2\text{‰}$  and exceeding the long-term average. Within this interval the highest  $\delta^{18}\text{O}$  values of  $>3.2\text{‰}$  are found between 300 and 170 cm ( $\sim 1350\text{ CE} - 1580\text{ CE}$ ). 5) Finally, the  $\delta^{18}\text{O}$



record becomes lower again ( $\sim 2.4\%$ ) between 53.5 and 5 cm ( $\sim 1900$  and 1996 CE). We did not find enough specimens of *Cassidulina laevigata* to perform isotopic analyses for samples between 5 and 0 cm (1996-1999).

Shifts of  $\sim 0.25\%$  in  $\delta^{18}\text{O}_c$  occur throughout the Gullmar Fjord  $\delta^{18}\text{O}$  record, which according to the used herein McCorkle et al. (1997) equation may potentially indicate a temperature variability of  $\sim 1^\circ\text{C}$ . A corresponding salinity change is rather small (0.02), calculated using the mixing line by Fröhlich et al. (1988) and by applying the  $\delta^{18}\text{O}_c$  range of 2.6-2.85 and a corresponding temperature range of 4.9-5.9 $^\circ\text{C}$ . Such salinity changes are well within the amplitude of inter-annual variability (1-1.5), recorded by instrumental salinity observations since the 1890 (Fig. 2). Foraminifera precipitate their tests during several months (e.g. Filipsson et al., 2004) and thus integrate the inter-monthly salinity signal, which together with annual variability is minimal according to the instrumental data. For the upper part of the record 1-cm sediment slice integrates one or possibly two growing seasons of *C. laevigata* and, hence, records a potentially higher variability of both salinity and temperature. In the deepest part of the record, however, a single 1-cm sample may correspond to  $\sim 7$ -10 years and, thus, more likely averages inter-annual salinity and temperature variability providing “a more smoothed” signal.

Stable carbon isotopes ( $\delta^{13}\text{C}$ ) data from the composite G113-2Aa – 9004 record (Filipsson and Nordberg, 2010) were plotted against the oxygen isotope data presented herein, to investigate the potential relationship between the two e.g. due to different water masses (Suppl. Fig. 1). No such relationship was found (Suppl. Fig. 1), which indicates that our  $\delta^{18}\text{O}$  record mainly reflects fjord deep-water temperatures.

#### 4.3 Reconstructed bottom water temperatures (BWTs)

The resulting calculated bottom water temperature record is plotted as both as absolute temperature values (Fig. 5) and as anomaly from the mean value (5.4 $^\circ\text{C}$ ), based on the instrumental temperatures observed between 1961 and 1990 (Fig. 6). With very few outliers, the reconstructed temperature range (2.7 - 7.8 $^\circ\text{C}$ ) is within the present-day annual variability, documented from instrumental temperature measurements in the fjord deepest basin since 1890 (Fig. 2A-C). Observed annual temperatures registered between 1890 and 1996 (which corresponds to the uppermost part of the composite G113-2Aa – 9004 record) vary between 3.0 and 8.3 $^\circ\text{C}$ , which gives an amplitude of 5.3 $^\circ\text{C}$ . Corresponding instrumental 1890-1996 temperatures for foraminiferal growth season (April-August) show a 3.0 - 7.2 $^\circ\text{C}$  range with an amplitude of 4.2 $^\circ\text{C}$ . When studying the reconstructed temperatures over the last 2500 years the corresponding amplitude, i.e. the difference between the maximum (7.8 $^\circ\text{C}$ ) and the minimum (2.7 $^\circ\text{C}$ ) temperatures is 5.1 $^\circ\text{C}$  (Fig. 5). Also when plotting the reconstructed bottom water temperatures for the period 1890 –1999 versus corresponding instrumental bottom water temperatures as annual average and means for May-August (Fig. 7B) and January-March (Fig. 7C), the calculated bottom water temperatures and hydrographic data agree with each other rather well in terms of amplitude. An increased agreement, however, is reached when comparing the reconstructed data to the hydrographic winter (Jan-March) temperature (Fig. 7C), which is not surprising considering the fjord hydrography and a season when deep-water exchanges typically occur (see Study Area



section). Hence, Gullmar Fjord  $\delta^{18}\text{O}$ -based temperature record reflects the winter temperature variability of surface water in the North Sea.

From the reconstructed Gullmar Fjord temperature record five bottom water temperature intervals can be recognized (Figs 5-6), in parallel to the isotopic intervals mentioned above. 1) From ~350 BCE to 450 CE the fjord bottom water temperatures are consistently above 5.4°C, the 1961-1990 mean. 2) Between 450 CE and 850 CE the record fluctuates between positive temperature anomalies (~450–650 CE) and negative anomalies (~650 – 850 CE) reaching minimum value at ~750 CE. 3) At ~850–1300 CE the bottom water temperatures are again above the average with a short negative anomaly around 1200-1250CE. 4) The period between ~1300 CE and 1850 CE in the Gullmar Fjord record is unprecedentedly cold for the last ~2500 years with the majority of temperature anomalies being negative and reaching the minimum value around ~1350 CE (Fig. 6). 5) Finally, from ~1850 CE towards present day the record is characterised by consistently positive bottom water temperature anomalies, which is comparable in the amplitude to the high anomalies found at ~350 BCE – 450 CE.

#### 4.4 Gaps in the record due to absent/rare *Cassidulina laevigata*

Some intervals in the G113-2Aa - 9004 record were barren of *C. laevigata* tests and hence for those intervals  $\delta^{18}\text{O}$  values and the corresponding reconstructed bottom water temperature data are missing. Those intervals are: ~130-120 BCE, ~725-740 CE, ~1260-1265 CE, ~1273-1277 CE, ~1340 CE and ~1996-1999 (Fig. 6). The most recent period of absent/rare *C. laevigata* in the Gullmar Fjord coincides with higher bottom water temperatures and frequently occurring severe hypoxia, as registered by the instrumental measurements in the deepest basin (Fig. 2C).

## 5 Discussion

The Gullmar Fjord winter bottom water temperature record shows both centennial and multidecadal variability and has a striking resemblance with historically known climate variations in northern Europe over the last 2500 years (e.g. Lamb 1995; Moberg et al., 2005; Filipsson and Nordberg, 2010; Helama et al., 2017). The record demonstrates periods of temperature variability, which correspond to the Roman Warm Period (~350 BCE – 450 CE), the Dark Ages cold period (~450 – 850 CE), the warm Viking Age/Medieval Climate Anomaly (~850 – 1350 CE), the colder Little Ice Age (~1350 – 1850 CE) as well as the warmer conditions during the 20<sup>th</sup> century (~1850 CE –present). There is an overall cooling trend in the Gullmar Fjord temperature record for the last 2500 years, which is consistent with other climate proxy records for this period (e.g. Lebreiro et al., 2006; Eiriksson et al., 2006; Hald et al., 2011; McGregor et al., 2015). Among forcing mechanisms for the late Holocene climate variability in the North Atlantic region changes in temperature and influx of the Atlantic Water to the region (e.g. Nordberg, 1991; Hass, 1996; Klitgaard-Kristensen et al., 2004; Eiriksson et al., 2006; Lund et al., 2006), radiative forcing (Jiang et al., 2005; Hald et al., 2007), volcanic activity (Otterå et al., 2010; McGregor et al., 2015) and land-



use changes (Abram et al., 2016) are suggested. In addition, there is a strong coupling between atmospheric - and ocean circulation linked to the variability of the North Atlantic Oscillation (NAO), where the NAO index is defined as the normalized sea level pressure difference between the Icelandic Low and the Azores High (Hurrell et al., 1995). The NAO influences strength and frequency of moist westerly winds, bringing precipitation to the Northern Europe and has even been suggested to induce multidecadal-scale changes in the North Atlantic thermohaline circulation (Dickson et al., 1996), which on centennial scales is linked to the late Holocene major climate extremes (Bianchi and McCave, 1999). Below we discuss each of the climate extremes in detail and compare our record to available temperature proxy data from other settings, highly influenced by the multidecadal NAO variability and climate changes associated with it.

### 5.1 The Roman Warm Period (prior to ~ 450 CE)

The fjord record shows consistently positive bottom water temperature anomalies during the Roman Warm Period (RWP) when compared to 5.4°C, the annual mean for 1961-1999 (Fig. 6). The RWP is often associated with increasingly warm and dry summers both on the British Isles and in the central Europe and is linked to the expansion of the Roman Empire (Lamb, 1995; Wang et al., 2012). The RWP warming coincided with a more vigorous flow of the Iceland Scotland Overflow Water, which is an important component of the AMOC modulating the European climate (Bianchi and McCave, 1999). Harland et al (2013) analysed dinoflagellate cysts from the same composite core as presented herein and, based on observed changes in species composition, suggested that sea surface temperatures (SSTs) in the fjord were >10°C during the RWP, as compared to the present-day SSTs of ~9°C (SMHI, 2017). Other studies suggest SSTs of 6-10°C for the waters off N Iceland (Sicre et al., 2011), 10.7-12.6°C for the Vøring Plateau, Norwegian Sea (Risebrobakken et al., 2011), >13°C for off the NW Scotland (Wang et al., 2012) and >15°C for the Rockall Trough, NE Atlantic (Richter et al., 2009) during this period. Also for the coastal NW Atlantic (Chesapeake Bay) the SSTs as high as 12-15°C were reported (Cronin et al., 2003).

For the adjacent Skagerrak an increase in both intermediate and bottom water temperatures is reported based on Mg/Ca data on benthic *Melonis barleeanus* by Butruille et al. (2017). The authors demonstrate a ~2°C temperature increase and report a temperature range of ~6-8°C during the RWP. In a 2000-yr long temperature record from the Malangen Fjord, NW Norway (Hald et al., 2011), the RWP is characterized as “a warm period with stable bottom water temperatures”. The Malangen fjord record is based on  $\delta^{18}\text{O}$  measured on *Cassidulina neoteretis* and documents a bottom water temperature range of 5.5-7.5°C (Hald et al., 2011). Both Skagerrak and Malangen Fjord studies agree well with our dataset, which demonstrates a temperature increase of ~2.5°C, resulting in a 5.4-7.9°C temperature range during the RWP for the Gullmar Fjord deep water (Fig. 5). The somewhat higher upper range limit of the RWP bottom water temperatures in the Skagerrak and Malangen Fjord, compared to our data, may be explained by a more direct influence of the more temperate Atlantic water at those sites, which is less obvious for our study area as it is more land-locked and with a stronger continental influence.



When comparing our data to the major temperature synthesis efforts done for the last two millennia, it becomes evident that our RWP reconstruction seem to disagree with the northern hemisphere temperature record of Moberg et al (2005), which is mostly characterized by the negative RWP temperature anomalies (Fig. 6). On the other hand, the warming seen in the Gullmar Fjord dataset is consistent with the PAGES2k temperature synthesis for the continental Europe (Fig. 6), which also reports a distinct warming corresponding to ~2-3°C temperature increase during the RWP (PAGES2k, 2013).

### 5.2 The Dark Ages Cold Period (~ 450 – 850 CE)

Our record displays variable bottom water temperatures in the fjord during the Dark Ages (Figs 5-6), which is initiated with a short-living negative anomaly at ~ 400-450 CE, then switches to positive values (~450-650 CE) and then becomes negative again at ~650-850 CE. The Dark Ages Cold Period (DACP) is commonly linked to a massive migration of the peoples in the central Europe (Lamb, 1995; Büntgen et al., 2011). The DACP was contemporaneous with a reduced flow of the Iceland Scotland Overflow Water (Bianchi and McCave, 1999), low solar activity, low pollen influx (Desprat et al., 2003) and glacier advance (Lamb, 1995). Summer temperatures <10°C in French Alps (Millet et al., 2009), increased humidity in the northern Europe (Barber et al., 2004) as well as a widespread abandonment of arable lands and cultivation in the SW Norway (Salvesen, 1979) were also documented for this period.

There is also some cooling during the DACP indicated for the intermediate and deep water in the adjacent Skagerrak (Butruille et al., 2017) but different temporal resolution makes it difficult to directly compare the Skagerrak record with ours. In contrast, variable SSTs during the Dark Ages are reported by some North Atlantic records (Sicre et al., 2011; Risebrobakken et al., 2011), with timing similar to the variability of the Gullmar temperatures (see above). Variable bottom water temperatures are also reported for the Malangen Fjord with a range (5.5-7.5°C) relatively close to our results (~4-8°C). There is also some fluctuation between cooling and warming with a ~3-4°C amplitude in a Mg/Ca -based SST record from the Chesapeake Bay (Cronin et al., 2003), as well as in the DACP temperatures reconstructed for the continental Europe (PAGES2k, 2013).

### 5.3 The Viking Age / Medieval Climate Anomaly (~ 850 – 1350 CE)

After the Dark Ages the bottom water temperature anomalies in Gullmar Fjord become positive between ~ 850 CE and 1350 CE, which fits well with the onset of the warming during the VA/MCA. The warm MCA is believed to be associated with a positive NAO index (e.g. Trouet et al., 2009; Faust et al., 2016), which likely have strengthened the AMOC (Bianchi & McCave, 1999) and resulted in an increased transport of heat and moisture to the higher latitudes. The MCA also coincided with Grand Solar Maximum at 1100–1250 CE (Zicheng and Ito, 2000) and its temperature optimum occurred between 1000 CE and 1300 CE when there was a sharp temperature maximum in most of Europe (Lamb, 1995).

The mean annual northern hemispheric and continental Europe temperature records (Moberg et al., 2005; PAGES2k, 2013) show the onset of warming as early as between ~850 and 950 CE, with distinct warmth peaks reached around 1000 CE



and 1100 CE and the MCA termination around 1300 CE, which all agrees with our data rather well (Fig. 6). The Malangen Fjord record also shows the warming already before 800 CE, which terminates around 1250 CE (Hald et al., 2011), a century earlier than in the Gullmar Fjord record. Despite such inconsistency in timing, which likely results from dating uncertainties (which may be the case for both studies), the two fjord records agree with each other rather well in terms of reconstructed bottom water temperature ranges for this period: 5.4-7.6°C for the Gullmar Fjord and 5.5-7.1°C for the Malangen Fjord. In the adjacent Skagerrak both intermediate and deep-water temperatures are reported to increase from ~6 to 8°C (Butruille et al., 2017) but sampling resolution of the former is too low for the MCA period. In turn, bottom water temperatures in the Scottish Loch Sunart also increased by ~1.2°C during the MCA (Cage and Austin, 2010), which is also within the abovementioned ranges. An increase of similar magnitude during the MCA is also reported for the sea surface temperatures in the North Atlantic (Cunningham et al., 2013).

An interesting feature in the Gullmar Fjord record of the VA/MCA is a presence of a short-lived cooling centred at ~1250 CE before the final peak of warmth at 1250-1350 CE (Fig. 6). Such short cooling during the MCA is also documented for both eastern and western Atlantic coasts (Chesapeake Bay: Cronin et al., 2003; Loch Sunart: Cage and Austin, 2010) but with a slightly different timing, either due to dating uncertainties or application of different temperature proxies (Mg/Ca vs  $\delta^{18}\text{O}$ ).

#### 5.4 The Little Ice Age (~1350 – 1850 CE)

From ~1350 CE to ~1850 CE our record shows winter bottom water temperatures 2-3°C lower than the instrumental annual mean for 1961-1999 (Fig. 6). Many other proxy records report cooling of similar magnitude or even stronger in the North Atlantic during the LIA (e.g. Cronin et al., 2003; Klitgaard Kristensen et al., 2004; Eiriksson et al., 2006; Hald et al., 2011; Sicre et al., 2011). The PAGES2k synthesis of marine palaeoclimate records spanning the past 2000 years also identified a robust global surface ocean cooling with the coldest conditions from 1400 to 1800 CE (Mcgregor et al., 2015). The Little Ice Age is commonly associated with glacier advances in the Arctic and alpine regions (Porter, 1986; Miller et al., 2012) in response to reduced solar activity (Mauquoy et al., 2002) and summer insolation (Wanner et al., 2011), increased volcanism (Miller et al., 2012), negative North Atlantic Oscillation (e.g. Trouet et al., 2009; Faust et al., 2016) and reduced strength of the AMOC (e.g. Bianchi & McCave, 1999; Klitgaard Kristensen et al., 2004; Lund et al., 2006). There is also a growing evidence for a stronger Siberian High prevailing from 1450 CE to 1900 CE based on increased  $\text{Na}^{2+}$  content in the GISP2 record from Greenland (Mayewski et al., 1997; Meeker and Mayewski, 2002). The onset of the LIA (~1350 CE) on the Swedish west coast also coincided in time with an outbreak of Black Death, which decreased the population by 50-60% and resulted in large-scale farm abandonment with negative implications for land use (Harrison, 2000).

For the Gullmar Fjord a general cooling during the LIA has been previously suggested based on increased abundances of cryophilic dinocysts (Harland et al., 2013) and benthic foraminifer *Adercotryma glomerata*, which prefers bottom water temperatures < 4°C (Polovodova Asteman et al., 2013). This agrees rather well with the data presented herein, which show



temperatures as low as  $\sim 3.4 - 4.4^{\circ}\text{C}$  around 1350 CE, 1500 CE, 1550 CE and 1700-1850 CE with a general temperature range of  $2.9-6.6^{\circ}\text{C}$  for the whole LIA period (Fig. 5). Based on foraminiferal faunal and  $\delta^{13}\text{C}$  data Polovodova Asteman et al. (2013) divided the LIA into two distinct phases in the Gullmar Fjord: 1) 1350–1650 CE and 2) 1650–1850 CE separated by a short-lived warming centred at  $\sim 1650$  CE. The reconstructed temperatures show as well a short milder episode based on

5 positive anomalies between  $\sim 1600$  and 1700 CE (Fig. 6). Similar warm, but slightly displaced in time, event is visible in other climate records (Fig. 6) from the North Atlantic and northern hemisphere (Cronin et al., 2003; Moberg et al., 2005; Cage and Austin, 2010; Hald et al., 2011) suggesting that this short-lived warming was a larger-scale phenomenon possibly linked to a strengthening of the winter NAO, which might have enhanced the AMOC (Cage and Austin, 2010).

The climax or the coldest part of the LIA is often linked to the Maunder minimum in solar activity, which occurred at

10  $\sim 1645-1715$  CE (Mauquoy et al., 2002). Our record shows a distinct cooling at around 1750 CE with temperatures  $\sim 1^{\circ}\text{C}$  below the 1961-1999 mean, which given a calibrated  $^{14}\text{C}$  age range for this particular date (1675-1813 CE  $\pm 25$  years: see Table 2), may well represent the Maunder minimum in our record. At the same time, a 500-yr long reconstruction of Stockholm winter temperatures based on sea ice records from local ports and harbours does not show the coldest temperatures during the LIA climax demonstrating instead that the coldest decade for the last 500 years occurred during

15 1592-1601 CE with average negative temperature anomalies of  $\sim -4^{\circ}\text{C}$  (Leijonhufvud et al., 2009).

It appears rather intriguing that the coldest bottom water temperatures for the last 2500 years in the Gullmar Fjord are associated with the onset of the LIA (1350 CE,  $\sim 2^{\circ}\text{C}$  colder than the 1961-1999 mean) rather than with its climax (Figs 5-6). This agrees well with the LIA temperature evolution reported for Loch Sunart (Cage and Austin, 2010) and Chesapeake Bay (Cronin et al., 2003), which both show  $2-4^{\circ}\text{C}$  cooling of the bottom waters at the MCA-LIA transition (Fig. 6), attributed to a

20 switch from the positive winter NAO mode dominating during the medieval times (e.g. Trouet et al., 2009; Faust et al., 2016) to the negative NAO prevailing during the major part of the Little Ice Age. Such a switch in the NAO has been linked to a relaxation of the persistent La-Niña – like conditions in the equatorial Pacific dominating the MCA (Trouet et al., 2009). The MCA-LIA transition has been dated to 1250 CE (Cunningham et al., 2013), 1400 CE (McGregor et al., 2015) and 1450 CE (Cage and Austin, 2010), in contrast to our study (1350 CE), which may again be a result of  $^{14}\text{C}$  dating uncertainties valid

25 for all of the above-mentioned marine records. At the same time the Chesapeake Bay study places MCA-LIA transition in between 1300 and 1400 CE (Cronin et al., 2003), which agrees with our data.

### 5.5 The Contemporary Warm Period ( $\sim 1850$ CE – present)

Most of the proxy records in the North Atlantic indicate a clear warming trend for the last 100-200 years (Hald et al., 2011 and references therein) similar to our data picking up the warm 1930s and the 1990s (Fig. 8). The 500-yr long reconstruction

30 of Stockholm winter temperatures also demonstrates that the 20<sup>th</sup> century has experienced four out of five warmest decades over the last 500 years: 1905-1914, 1930-1939, 1989-1998 and 1999-2008 (Leijonhufvud et al., 2009). Gullmar Fjord temperature record shows that when considering a 3-point running mean temperature variability, the most recent warming



stretching to 1999 does not stand out in comparison to the RWP and the MCA, similar to the Scottish loch data (Cage and Austin, 2010) and the North Atlantic SST composite (Cunningham et al., 2013) but in contrast to the Malangen Fjord record (Hald et al., 2011), according to which the last 100 years are the warmest in the last 2000 years. This may reflect the so-called polar amplification, as suggested by the authors, since Malangen Fjord is located much more to the north than Loch Sunart and Gullmar Fjord, both comparably temperate fjord inlets. At the same time the spring SST reconstruction from the Chesapeake Bay (Cronin et al., 2003, Fig. 6 herein) shows that the 20<sup>th</sup> century warming clearly exceeds the temperatures observed during the prior 2500 years. The shallow Chesapeake Bay displays large seasonal temperature and salinity variability (Cronin et al., 2003) in contrast to Gullmar Fjord, Malangen Fjord and Loch Sunart, which all have slightly/ less variable bottom water conditions during the year and similar “fjordic” circulation with annual or less frequent basin water exchanges. Also the SST record from the Chesapeake Bay is the shallowest temperature reconstruction (12-25 m w. d.) among the temperature records considered herein (Loch Sunart: 56 m; Gullmar Fjord: 120 m and Malangen Fjord: 218 m w. d.), which also may explain why its recent warming is unprecedented in a 2500-year perspective.

Studying the instrumental hydrographic time series from the fjord plotted versus reconstructed temperatures (Fig. 7) makes it clear that our record captures the most recent warm period with the bottom water temperatures, which increased by ~1.5°C since the 1960s. Similar increase has been documented for Loch Sunart (Cage and Austin, 2010) and Ranafjorden, NW coast of Norway (Klitgaard-Kristensen et al., 2004). Instrumental meteorological time series for air temperatures since 1960s from Stockholm and the Central England also demonstrate a winter temperature increase by 3-3.5°C, which is higher than the reconstructed range of Gullmar Fjord bottom water temperatures for this period (Fig. 8). Overall, the variability in reconstructed fjord temperatures corresponds well with both meteorological datasets from 1750 to 1990, by an exception of individual wiggle mismatch between 1930 and 1990 (Fig. 8). In general it appears that for 1930-1990 period both air temperatures records lead the observed variability while bottom water temperatures are lagging behind (Fig. 8).

Since 1990, however, *Cassidulina laevigata* has dramatically decreased in abundances in the Gullmar Fjord deep basin (Fig. 6). Similar pattern, with short extinctions of *C. laevigata*, is seen during the Roman and Medieval warm periods (Fig. 6).

This effect may be either due to the increased temperatures or, more likely, due to periods of severe hypoxia as *C. laevigata* appears to be sensitive to oxygen concentrations below 1 ml/l (e.g. Gustafsson & Nordberg 2001; Nardelli et al., 2014). To a large extent, the oxygen status of fjords and estuaries on the Swedish west coast, is controlled by climate (e.g. Nordberg et al., 2000; Filipsson and Nordberg 2004a, b), and the short extinctions of *C. laevigata* during warmer periods further back in time may be equivalent to the present-day pattern of severe hypoxia following positive North Atlantic Oscillation with mild and humid winters, limited basin water exchange and high organic matter flux increasing oxygen demand (Nordberg et al. 2000, 2001; Filipsson & Nordberg 2004a). Indeed, when comparing our record to the reconstructed NAO index from the Trondheim Fjord, W Norway (Faust et al., 2016) it appears that core intervals with absent *C. laevigata* (at ~75 CE, 450 CE, 1000 CE and post-1990) correlate rather well with the positive NAO index (Fig. 6).



## 6 Conclusions

To conclude, from the available paleotemperature equations, the equation by McCorkle et al (1997) produced most realistic reconstructed deep water temperature range of 2.7 - 7.8°C, which falls within the annual variability instrumentally recorded in the deep fjord basin since 1890. This suggests that the Gullmar Fjord  $\delta^{18}\text{O}$  record mainly reflects variability of the winter bottom water temperatures with a minor salinity influence. Comparison with instrumental winter temperature observations from Central England and Stockholm shows that the fjord record picks up the contemporary warming of the 20<sup>th</sup> century. The relationship between the evolution of the fjord's bottom water temperatures over the last two millennia and other late Holocene climate records reveals synchronous North Atlantic-wide centennial and multidecadal climate variability given age model uncertainties, different proxy type, time resolution, annual versus seasonal signal and different hydrographic characteristics.

The record shows a substantial and long-term warming during the Roman Warm Period (~350 BCE – 450 CE), followed by variable bottom water temperatures during the Dark Ages (~450 – 850 CE). The Viking Age/Medieval Climate Anomaly (~850 – 1350 CE) is also indicated by positive bottom water temperature anomalies, while the Little Ice Age (~1350 – 1850 CE) is characterized by a long-term cooling with distinct multidecadal variability. When studying the Gullmar Fjord bottom water temperature record for the last 2500 years, it is interesting to note that the most recent warming of the 20<sup>th</sup> century does not stand out but appears to be comparable to both the Roman Warm Period and the MCA.

## Data availability

The data for this paper are available at [www.pangaea.de](http://www.pangaea.de).

## 20 Author contribution

KN conceived the research, obtained funding, as well as, organized and performed sediment core sampling in 1990 and 1999. HLF participated in the 1999 cruise; together with KN prepared samples for stable oxygen isotopes, funded isotope analysis and collected the data. All authors contributed to data analysis & interpretation. IPA wrote the manuscript with the help of both co-authors.

## 25 Competing interests

The authors declare that they have no conflict of interests.



### Acknowledgements

The crews of R/V Svanic, R/V Arne Tiselius and R/V Skagerak helped with sampling. The study was financed by the Swedish Research Council: VR grants no 621-2004-5320, 621-2007-4369 (KN) and 621-2005-4265 (HLF); Lamm Foundation (KN); University of Gothenburg (KN); Marine Research Centre, GMF (KN), and EUROPROX - European Graduate College – Proxies in Earth History (HLF). Monika Segl (University of Bremen) measured stable O and C isotopes. The PALEOSTUDIES program (University of Bremen) covered the costs for isotope analyses, while the Department of Earth Sciences (University of Gothenburg) provided a postdoctoral fellowship to IPA.

### References

- Abram, N. J., McGregor, H. V., Tierney, J. E., Evans, M. N., McKay, N. P., Kaufman, D. S., & PAGES 2k Consortium.:  
10 Early onset of industrial-era warming across the oceans and continents. *Nature*, 536 (7617), 411-418, 2016.
- Appleby, P. G., & Oldfield, F.: The calculation of lead-210 dates assuming a constant rate of supply of unsupported 210Pb to the sediment. *Catena*, 5(1), 1-8, 1978.
- Arneborg, L.: Turnover times for the water above sill level in Gull- mar Fjord, *Cont. Shelf Res.*, 24, 443–460, 2004.
- Barber, K.E., Chambers, F.M., Maddy, D.: Late Holocene climatic history of northern Germany and Denmark: peat  
15 macrofossil investigations at Dosenmoor, Schleswig– Holstein and, Svanemose, Jutland. *Boreas* 33, 132–144, 2004.
- Bemis, B. E., Spero, H. J., Bijma, J., & Lea, D. W.: Reevaluation of the oxygen isotopic composition of planktonic foraminifera: Experimental results and revised paleotemperature equations. *Paleoceanography*, 13(2), 150-160, 1998.
- Bianchi, G. G., & McCave, I. N.: Holocene periodicity in North Atlantic climate and deep-ocean flow south of Iceland. *Nature*, 397 (6719), 515-517, 1999.
- 20 Björk, J. & Nordberg, K.: Upwelling along the Swedish west coast during the 20th century, *Cont. Shelf Res.*, 23, 1143–1159, 2003.
- Bronk Ramsey, C.: Improving the resolution of radiocarbon dating by statistical analysis, in: *Radiocarbon Dating: Archaeology, Text and Science*, edited by: Levy, T. E. and Higham, T. F. G., The Bible and Equinox, London, 57–64, 2005.
- 25 Butler, P. G., Wanamaker, A. D., Scourse, J. D., Richardson, C. A., & Reynolds, D. J.: Variability of marine climate on the North Icelandic Shelf in a 1357-year proxy archive based on growth increments in the bivalve *Arctica islandica*. *Palaeogeography, Palaeoclimatology, Palaeoecology*, 373, 141-151, 2013.
- Butruille, C., Krossa, V. R., Schwab, C., & Weinelt, M.: Reconstruction of mid-to late-Holocene winter temperatures in the Skagerrak region using benthic foraminiferal Mg/Ca and  $\delta^{18}\text{O}$ . *The Holocene*, 27(1), 63-72, 2017.
- 30 Büntgen, U., Tegel, W., Nicolussi, K., McCormick, M., Frank, D., Trouet, V., Kaplan, J. O., Herzig, F., Heussner, K. U., Wanner, H., Luterbacher, J., and Esper, J.: 2500 Years of European Cli- mate Variability and Human Susceptibility, *Science*, 331, 578– 582, 2011.



- Cage, A. G. and Austin, W. E. N.: Marine climate variability during the last millennium: the Loch Sunart record, Scotland, UK, *Quaternary Sci. Rev.*, 29, 1633–1647, 2010.
- Cronin, T.M., Dwyer, G.S., Kamiya, T., Schwede, S., Willard, D.A.: Medieval Warm Period, Little Ice Age and 20<sup>th</sup> century variability from Chesapeake Bay. *Glob. Planet. Change* 36, 17–29, 2003.
- 5 Cunningham, L. K., Austin, W. E., Knudsen, K. L., Eiriksson, J., Scourse, J. D., Wanamaker Jr, A. D., Butler, P.G., Cage, A.G., Richter, T., Husum, K., Hald, M., Andersson, C., Zorita, E., Linderholm, H.W., Gunnarsson, B., Sicre, M.-A., Sejrup, H.P., Jiang, H. & Wilson, R.J.S.: Reconstructions of surface ocean conditions from the northeast Atlantic and Nordic seas during the last millennium. *The Holocene*, 23(7), 921–935, 2013.
- Desprat, S., Goñi, M. F. S., & Loutre, M. F.: Revealing climatic variability of the last three millennia in northwestern Iberia using pollen influx data. *Earth and Planetary Science Letters*, 213(1), 63–78, 2003.
- 10 Dickson, R., Lazier, J., Meincke, J., Rhines, P., Swift, J.: Long-term coordinated changes in the convective activity of the North Atlantic. *Prog. Oceanogr.* 38, 241–295, 1996.
- Eiriksson, J., Bartels-Jonsdottir, H. B., Cage, A. G., Gudmundsdottir, E. R., Klitgaard-Kristensen, D., Marret, F., Rodrigues, T., Abrantes, F., Austin, W.E.N., Jiang, H., Knudsen, K. L. & Sejrup, H.P.: Variability of the North Atlantic Current during the last 2000 years based on shelf bottom water and sea surface temperatures along an open ocean/shallow marine transect in western Europe. *The Holocene*, 16(7), 1017–1029, 2006.
- 15 Faust, J. C., Fabian, K., Milzer, G., Giraudeau, J., & Knies, J.: Norwegian fjord sediments reveal NAO related winter temperature and precipitation changes of the past 2800 years. *Earth and Planetary Science Letters*, 435, 84–93, 2016.
- Filipsson, H. L. and Nordberg, K.: Variations in organic carbon flux and stagnation periods during the last 2400 years in a Skagerrak fjord basin, inferred from benthic foraminiferal  $\delta^{13}C$ , in: *Fjords: Depositional Systems and Archives*, Geological Society Special Publication, edited by: Howe, J. A., Austin, W. E. N., Forwick, M., Powell, R. D., and Paetzel, M., 261–270, 2010.
- 20 Filipsson, H. L., & Nordberg, K.: Climate variations, an overlooked factor influencing the recent marine environment. An example from Gullmar Fjord, Sweden, illustrated by benthic foraminifera and hydrographic data. *Estuaries*, 27(5), 867–881, 2004a.
- 25 Filipsson, H. L., & Nordberg, K.: A 200-year environmental record of a low-oxygen fjord, Sweden, elucidated by benthic foraminifera, sediment characteristics and hydrographic data. *Journal of Foraminiferal Research*, 34(4), 277–293, 2004b.
- Filipsson, H. L., Bernhard, J. M., Lincoln, S. A., & McCorkle, D. C.: A culture-based calibration of benthic foraminiferal paleotemperature proxies: delta O-18 and Mg/Ca results. *Biogeosciences*, 7, 1335–1347, 2010.
- 30 Frohlich, K., Grabczak, J., & Rozanski, K.: Deuterium and oxygen-18 in the Baltic Sea. *Chemical Geology: Isotope Geoscience Section*, 72(1), 77–83, 1988.
- Gunnarson, B. E., Linderholm, H. W., and Moberg, A.: Improving a tree-ring reconstruction from west-central Scandinavia: 900 years of warm-season temperatures, *Clim. Dynam.*, 36, 97–108, 2011.



- Gustafsson, M. and Nordberg, K.: Living (stained) benthic foraminiferal response to primary production and hydrography in the deepest part of the Gullmar Fjord, Swedish West Coast, with comparisons to Høglund's 1927 material, *J. Foramin. Res.*, 31, 2–11, 2001.
- Hald, M., Salomonsen, G. R., Husum, K., & Wilson, L. J.: A 2000-year record of Atlantic Water temperature variability from the Malangen Fjord, northeastern North Atlantic. *The Holocene*, 21(7), 1049–1059, 2011.
- 5 Hald, M., Andersson, C., Ebbesen, H., Jansen, E., Klitgaard-Kristensen, D., Risebrobakken, B., Salomonsen, G.R., Sarnthein, M., Sejrup, H.P., Telford, R. J.: Variations in temperature and extent of Atlantic Water in the northern North Atlantic during the Holocene. *Quaternary Science Reviews*, 26(25), 3423–3440, 2007.
- Harrison, D.: *Stora Döden/ The Black Death*, Stockholm, Ordfront, 2000 (in Swedish).
- 10 Harland, R., Polovodova Asteman, I., Nordberg, K.: A two-millennium dinoflagellate cyst record from Gullmar Fjord, a Swedish Skagerrak sill fjord. *Palaeogeography, Palaeoclimatology, Palaeoecology* 392, 247–260, 2013.
- Harland, R., Nordberg, K., & Filipsson, H. L.: Dinoflagellate cysts and hydrographical change in Gullmar Fjord, west coast of Sweden. *Science of the total environment*, 355(1), 204–231, 2006.
- Hass, H. C.: Northern Europe climate variations during late Holocene: evidence from marine Skagerrak, *Palaeogeogr. Palaeoclimatol.*, 123, 121–145, 1996.
- 15 Hays, P.D. & Grossman, E.L.: Oxygen isotopes in meteoric calcite cements as indicators of continental paleoclimate. *Geology* 19, 441–444, 1991.
- Helama, S., Jones, P.D., Briffa, K.R.: Dark Ages Cold Period: a literature review and directions for future research. *The Holocene* 27(10), 1600–1606, 2017.
- 20 Howe, J. A., Austin, W. E. N., Forwick, W., Paetzel, M., Harland, R., and Cage, A. G.: Fjord systems and archives: a review, in: *Fjords: Depositional Systems and Archives*, edited by: Howe, J. A., Austin, W. E. N., Forwick, M., and Paetzel, M., Geological Society Special Publication, 261–270, 2010.
- Hurrell, J.W.: Decadal trends in the north-Atlantic oscillation – regional temperatures and precipitation. *Science* 269 (5224), 676–679, 1995.
- 25 Kjennbakken, H., Sejrup, H. P., & Haflidason, H.: Mid-to late-Holocene oxygen isotopes from Voldafjorden, western Norway. *The Holocene*, 21(6), 897–909, 2011.
- Klitgaard-Kristensen, D., Sejrup, H. P., Haflidason, H., Berstad, I. M., & Mikalsen, G.: Eight-hundred-year temperature variability from the Norwegian continental margin and the North Atlantic thermohaline circulation. *Paleoceanography*, 19(2), 2004.
- 30 Jiang, H., Eiriksson, J., Schulz, M., Knudsen, K. L., & Seidenkrantz, M. S.: Evidence for solar forcing of sea-surface temperature on the North Icelandic Shelf during the late Holocene. *Geology*, 33(1), 73–76, 2005.
- Lamb, H. H.: *1977 Climate: present, past and future*. New York: Methuen, 1995.
- Lamb, H. H.: Some studies of the Little Ice Age of recent centuries and its great storms, in: *Climatic changes on a yearly to*



- millen- nial basis: Geological, historical and instrumental records, edited by: Mörner, N. A. and Karlén, W., D. Reidel Publishing Company, Dordrecht, 1983.
- Lebreiro, S. M., Francés, G., Abrantes, F. F. G., Diz, P., Bartels-Jónsdóttir, H. B., Stroynowski, Z. N., Gil, I.M., Pena, L.D., Rodrigues, T., Jones, P.D., Nombella, M.A., Alejo, I., Briffa, K.R., Harris, I., Grimalt, J.O.: Climate change and coastal hydrographic response along the Atlantic Iberian margin (Tagus Prodelta and Muros Ría) during the last two millennia. *The Holocene*, 16(7), 1003-1015, 2006.
- Leijonhufvud, L., Wilson, R., Moberg, A., Soderberg, J., Retso, D., and Soderlind, U.: Five centuries of Stockholm winter/spring temperatures reconstructed from documentary evidence and instrumental observations, *Climatic Change*, 101, 109–141, 2010.
- 10 Linderholm, H.W., Björklund, J., Seftigen, K., Gunnarson, B. E., & Fuentes, M.: Fennoscandia revisited: a spatially improved tree-ring reconstruction of summer temperatures for the last 900 years. *Climate Dynamics*, 45(3-4), 933-947, 2015.
- Lund, D. C., Lynch-Stieglitz, J., and Curry, W. B.: Gulf Stream density structure and transport during the past millennium, *Nature*, 444, 601–604, 2006.
- 15 Mann, M. E., & Jones, P. D.: Global surface temperatures over the past two millennia. *Geophysical Research Letters*, 30(15), 2003.
- Marchitto, T. M., Curry, W. B., Lynch-Stieglitz, J., Bryan, S. P., Cobb, K. M., & Lund, D. C.: Improved oxygen isotope temperature calibrations for cosmopolitan benthic foraminifera. *Geochimica et Cosmochimica Acta*, 130, 1-11, 2014.
- Mauquoy, D., van Geel, B., Blaauw, M., and van der Plicht, J.: Evidence from northwest European bogs shows “Little Ice Age” climatic changes driven by variations in solar activity, *The Holocene*, 12, 1–6, 2002.
- 20 Mayewski, P.A., Meeker, L.D., Twickler, M.S., Whitlow, S., Yang, Q.Z., Lyons, W.B., Prentice, M.: Major features and forcing of high-latitude northern hemisphere atmospheric circulation using a 110,000-year-long glaciochemical series. *Journal of Geophysical Research-Oceans* 102 (C12), 26345–26366, 1997.
- McCorkle, D. C., Corliss, B. H., & Farnham, C. A.: Vertical distributions and stable isotopic compositions of live (stained) benthic foraminifera from the North Carolina and California continental margins. *Deep Sea Research Part I: Oceanographic Research Papers*, 44(6), 983-1024, 1997.
- 25 McDermott, F., Matthey, D. P., & Hawkesworth, C.: Centennial-scale Holocene climate variability revealed by a high-resolution speleothem  $\delta^{18}\text{O}$  record from SW Ireland. *Science*, 294 (5545), 1328-1331, 2001.
- 30 McGregor, H. V., Evans, M. N., Goosse, H., Leduc, G., Martrat, B., Addison, J. A., Mortyn, P.G., Oppo, D.W., Seidenkrantz, M.-S., Sicre, M.-A., Phipps, S. J., Selvaraj, K., Thirumalaj, K., Filipsson, H. & Ersek, V.: Robust global ocean cooling trend for the pre-industrial Common Era. *Nature Geoscience*, 2015.
- Meeker, L.D., Mayewski, P.A.: A 1400-year high-resolution record of atmospheric circulation over the North Atlantic and Asia. *Holocene* 12 (3), 257–266, 2002.



- Mikalsen, G., Sejrup, H. P., & Aarseth, I.: Late-Holocene changes in ocean circulation and climate: foraminiferal and isotopic evidence from Sulafjord, western Norway. *The Holocene*, 11(4), 437-446, 2001.
- Miller, G. H., Geirsdottir, A., Zhong, Y. F., Larsen, D. J., Otto-Bliesner, B. L., Holland, M. M., Bailey, D. A., Refsnider, K. A., Lehman, S. J., Southon, J. R., Anderson, C., Bjornsson, H., and Thordarson, T.: Abrupt onset of the Little Ice Age triggered by volcanism and sustained by sea-ice/ocean feedbacks, *Geophys. Res. Lett.*, 39, L02708, doi:10.1029/2011GL050168, 2012.
- Millet, L., Arnaud, F., Heiri, O., Magny, M., Verneaux, V., Desmet, M.: Late-Holocene summer temperature reconstruction from chironomid assemblages of Lake Anterne, northern French Alps. *Holocene* 19, 317–328, 2009.
- Moberg, A., Sonechkin, D. M., Holmgren, K., Datsenko, N. M., and Karlén, W.: Highly variable Northern Hemisphere temperatures reconstructed from low- and high-resolution proxy data, *Nature*, 433, 613–617, 2005
- Morris, C.D.: Viking Orkney: a survey. In: Renfrew, C. (Ed.), *The Prehistory of Orkney*. Edinburgh University Press, Edinburgh, 1985.
- Nardelli, M. P., Barras, C., Metzger, E., Mouret, A., Filipsson, H. L., Jorissen, F., & Geslin, E.: Experimental evidence for foraminiferal calcification under anoxia. *Biogeosciences*, 11(14), 4029-4038, 2014.
- Nordberg, K.: Oceanography in the Kattegat and Skagerrak over the past 8000 years. *Paleoceanography* 6 (4), 461-484, 1991
- Nordberg, K., Gustafsson, M., and Krantz, A. L.: Decreasing oxygen concentrations in the Gullmar Fjord, Sweden, as confirmed by benthic foraminifera, and the possible association with NAO, *J. Marine Syst.*, 23, 303–316, 2000.
- Nordberg, K., Filipsson, H.L., Linné, P. and Gustafsson, M.: Stable isotope evidence for the recent establishment of a new, opportunistic foraminiferal fauna within Gullmar Fjord, Sweden. *J. Mar. Micropal.* 73, 117-128, 2009.
- O'Neil, J.R., Clayton, R.N., and Mayeda, T.K.: Oxygen isotope fractionation in divalent metal carbonates: *Journal of Chemical Physics*, 51, 5547-5558, 1969.
- Otterå, O. H., Bentsen, M., Drange, H., & Suo, L.: External forcing as a metronome for Atlantic multidecadal variability. *Nature Geoscience*, 3(10), 688-694, 2010.
- PAGES 2K Consortium: Continental scale temperature variability during the past two millennia. *Nature Geosciences* 6, 339-982, 2013.
- PAGES 2K Consortium: Data descriptor: A global multiproxy database for temperature reconstructions of the common era. *Nature Scientific Data* 4: 170088, DOI:10.1038/sdata.2017.88, 2017.
- Park, W., & Latif, M.: Multidecadal and multicentennial variability of the meridional overturning circulation, *Geophys. Res. Lett.*, 35, L22703, doi:10.1029/2008GL035779, 2008.
- Pettersson, O. & Ekman, G.: Grunddragen af Skageracks och Kattegats hydrografi. Kongl. Svenska Vetenskaps-akademiens handlingar 24 (11) 130 pp., 1891.
- Polovodova Asteman, I. & Nordberg, K.: Foraminiferal fauna from a deep basin in Gullmar Fjord: the influence of seasonal hypoxia and North Atlantic Oscillation. *J. Sea Res.* 79, 40–49, 2013.



- Polovodova Asteman, I., Nordberg, K., Filipsson, H.L.: The Little Ice Age: evidence from a sediment record in Gullmar Fjord, Swedish west coast. *Biogeosciences* 10, 1275–1290, 2013.
- Polovodova, I., Nordberg, K., Filipsson, H.L.: The benthic foraminiferal record of the Medieval Warm Period and the recent warming in the Gullmar Fjord, Swedish west coast. *Mar. Micropaleontol.* 81, 95–106, 2011.
- 5 Poole, D.A.R., Dokken, T.M., Hald, M., and Polyak, L.: Stable isotope fractionation in recent benthic foraminifera from the Barents and Kara Seas. PhD, University of Bergen, 1994.
- Porter, S. C.: Pattern and forcing of Northern-Hemisphere glacier variations during the last millenium. *Quaternary Res.*, 26, 27–48, 1986.
- Reimer, P. J., Bard, E., Bayliss, A., Beck, J. W., Blackwell, P. G., Bronk Ramsey, C., Buck, C. E., Cheng, H., Edwards, R.  
10 L., Friedrich, M., Grootes, P. M., Guilderson, T. P., Hafliadason, H., Hajdas, I., Hatté, C., Heaton, T. J., Hoffman, D. L., Hogg, A. G., Hughen, K. A., Kaiser, K. F., Kromer, B., Manning, S. W., Niu, M., Reimer, R. W., Richards, D. A., Scott, E. M., Southon, J. R., Staff, R. A., Turney, C. S. M. & van der Plicht, J.: IntCal13 and Marine13 radiocarbon age calibration curves 0-50,000 years cal BP. *Radiocarbon* 55, 1869–1887, 2013.
- Reimer, P. J., Baillie, M. G. L., Bard, E., Bayliss, A., Beck, J. W., Bertrand, C. J. H., Blackwell, P. G., Buck, C. E., Burr, G.  
15 S., Cutler, K. B., Damon, P. E., Edwards, R. L., Fairbanks, R. G., Friedrich, M., Guilderson, T. P., Hogg, A. G., Hughen, K. A., Kromer, B., McCormac, G., Manning, S., Ramsey, C. Bronk, Reimer, R. W., Remmele, S., Southon, J. R., Stuiver, M., Talamo, S., Taylor, F. W., van der Plicht, J., and Weyhenmeyer, C. E.: Int- Cal04 terrestrial radiocarbon age calibration, 0–26 cal kyr BP, *Radiocarbon*, 46, 1029–1058, 2004.
- Richter, T. O., Peeters, F. J., & van Weering, T. C.: Late Holocene (0–2.4 kaBP) surface water temperature and salinity  
20 variability, Feni Drift, NE Atlantic Ocean. *Quaternary Science Reviews*, 28(19), 1941-1955, 2009.
- Risebrobakken, B., Dokken, T., Smedsrud, L. H., Andersson, C., Jansen, E., Moros, M., & Ivanova, E. V.: Early Holocene temperature variability in the Nordic Seas: The role of oceanic heat advection versus changes in orbital forcing. *Paleoceanography*, 26(4), PA4206, doi:10.1029/2011PA002117, 2011.
- Rydberg, L.: Circulation in the Gullmaren – a sill fjord with externally maintained stratification. *Inst. of Oceanography*,  
25 Univ. of Gothenburg, Report no: 23 (mimeo), Gothenburg, 1977.
- Salvesen, H.: *Jord i Jemtland. Östersund, AB Wisenska bokhandelens förlag*, 187 pp., 1979.
- Shackleton, N. J.: Attainment of isotopic equilibrium between ocean water and the benthonic foraminifera genus *Uvigerina*: isotopic changes in the ocean during the last glacial. *Colloques Internationaux du CNRS* nr. 219, 203-209, 1974.
- Sicre, M. A., Hall, I. R., Mignot, J., Khodri, M., Ezat, U., Truong, M. X., Eiriksson, J., and Knudsen, K. L.: Sea surface  
30 temperature variability in the subpolar Atlantic over the last two millennia, *Paleoceanography*, 26, PA4218, 2011.
- Sicre, M.-A., Weckström, K., Seidenkrantz, M.-S., Kuijpers, A., Benetti, M., Masse, G., Ezat, M., Schmidt, S., Bouloubassi, I., Olsen, J., Khodri, M., Mignot, J.: Labrador current variability over the last 2000 years. *Earth Planet. Sci. Lett.* 400, 26-32, 2014.
- Stuiver, M. and Pollach, H. A.: Discussions of reporting <sup>14</sup>C data, *Radiocarbon*, 19, 355–363, 1977.



- Stuiver, M., Reimer, P. J. & Reimer, R. W.: CALIB 7.1 [WWW program], 2017 at <http://calib.org>, accessed 2017-2-16.
- Svansson A : Physical and chemical oceanography of the Skagerrak and the Kattegat. I. Open Sea Conditions. *Institute of Marine Research*, Report No. 1. Lysekil: Fishery Board of Sweden, pp. 1–88, 1975
- Tarutani T., Clayton R. N. & Mayeda T. K.: The effect of polymorphism and magnesium substitution on oxygen isotope fractionation between calcium carbonate and water. *Geochim. Cosmochim. Acta* 33, 987–996, 1969.
- 5 Trouet, V., Esper, J., Graham, N. E., Baker, A., Scourse, J. D., and Frank, D. C.: Persistent Positive North Atlantic Oscillation Mode Dominated the Medieval Climate Anomaly, *Science*, 324, 78–80, 2009.
- Wang, T., Surge, D., Mithen, S.: Seasonal temperature variability of the Neoglacial (3300–2500 BP) and Roman Warm Period (2500–1600 BP) reconstructed from oxygen isotope ratios of limpet shells (*Patella vulgata*), Northwest  
10 Scotland. *Palaeogeogr. Palaeoclimatol. Palaeoecol.* 317–318, 104–113, 2012.
- Wanner, H., Solomina, O., Grosjean, M., Ritz, S. P., and Jetel, M.: Structure and origin of Holocene cold events, *Quaternary Sci. Rev.*, 30, 3109–3123, 2011.
- Zicheng, Y. & Ito, E.: Historical solar variability and midcontinent drought. *Pages Newsl.* 8, 6–7, 2000.

**Datasets used in this paper were extracted from:**

- 15 SMHI, SHARK database <https://www.smhi.se/klimatdata/oceanografi/havsmiljodata/marina-miljoovervakningsdata>,  
[accessed 15/03/2017](#).
- SMHI: Meteorological observations of air temperatures: <https://www.smhi.se/klimatdata>, [accessed 15/03/2017](#).
- ICES database: <http://www.ices.dk/marine-data/>, [accessed 08/03/2017](#).
- Central England air temperature dataset: <http://www.metoffice.gov.uk/>, [accessed 16/03/2017](#).

20

**Figure captions**

**Figure 1:** Map of the study area including location of Gullmar Fjord (GF) and sampling site of Gal13-2Aa & 9004 record (star) within North Atlantic (A) and North Sea – Skagerrak region (B). Locations of other relevant proxy records, discussed  
25 in the text, are shown by white circles. C: an overview of water column stratification in the longitudinal profile of the Gullmar Fjord with indication of salinity (S) and residence times (t) typical for each water layer (Arneborg, 2004).

**Figure 2:** Hydrographic measurements from Alsäck Deep, Gullmar Fjord taken during 1890 – 2000 below 110 m water depth: temperature (a), salinity (b) and dissolved oxygen (c). A snapshot of hydrographic changes in temperature (d), salinity  
30 (e) and oxygen (f) associated with basin water exchanges between 1992 and 1993 showing annual variability of these



parameters.

**Figure 3:** Age model of the studied Ga113-2Aa & 9004 record (A) and correlation of foraminiferal and isotopic data with core G113-091, taken at the same location in 2009, to prove the absence of a gap between GA113-2Aa and 9004 (B),  
5 according to Polovodova Asteman et al (2013).

**Figure 4:** Comparison of reconstructed temperatures and  $\delta^{18}\text{O}$  values measured in stained *C. laevigata* from the core tops collected in Gullmar Fjord (G113-091) and the Skagerrak (OS4, OS6, OS14, 9202, 9205) to hydrographic temperature data (A) and to  $\delta^{18}\text{O}$  predicted from palaeotemperature equation (B) by McCorkle et al (1997). C: Temperature vs.  $\delta^{18}\text{O}$  –  
10  $\delta^{18}\text{O}$ , together with the paleotemperature equations from Shackleton (1974), Hays and Grossman (1991), Kim and O'Neil (1997), McCorkle et al. (1997), and Bemis et al. (1998).

**Figure 5:** A 2500-year long  $\delta^{18}\text{O}$  record and reconstructed winter bottom water temperatures from Gullmar Fjord. Thick lines show 3-point running mean for both curves, and dashed lines indicate 1) a long-term average of 2.4‰ for  $\delta^{18}\text{O}$  record  
15 and 2) 5.4°C - a mean for instrumental bottom water temperatures registered between 1961 and 1990. Grey shaded areas in BWTs indicate a median offset (0.7°C) in instrumental versus reconstructed temperatures obtained for rose Bengal stained *C. laevigata* from the core tops (see Fig. 4A), used herein as an error margin.

**Figure 6:** Reconstructed bottom water temperatures (as anomaly against the 1961-1990 instrumental mean of 5.4°C) from  
20 Gullmar Fjord compared against other temperature proxy records: annual northern hemisphere temperatures (Moberg et al., 2005), bottom water temperatures from Malangen Fjord in NW Norway (Hald et al., 2011) and Loch Sunart in Scotland (Cage and Austin, 2010), spring sea surface temperatures from Chesapeake Bay, E North Atlantic Ocean (Cronin et al., 2003), annual temperatures reconstructed for continental Europe (Pages2K, 2013) and the reconstructed NAO record from Trondheim Fjord, W Norway (Faust et al., 2016). Also are shown relative abundances of foraminifer *Cassidulina laevigata*  
25 in the fjord with abundance minima and respective gaps in temperature reconstruction linked to the positive NAO index (arrows). For location of these proxy records see Fig. 1A. Grey shaded areas in Gullmar Fjord BWT anomalies indicate a median offset (0.7°C) in instrumental versus reconstructed temperatures (see Fig. 4A) obtained for rose Bengal stained *C. laevigata* from the core tops, used herein as an error margin.

30 **Figure 7:** Comparison of the winter bottom water temperatures reconstructed from Gullmar Fjord record to instrumental basin water temperatures measured in the deepest fjord basin: the annual mean (a), mean for May-August (b) and mean for January-March (c).



**Figure 8:** Comparison of the winter bottom water temperatures reconstructed from Gullmar Fjord record to meteorological observations of winter air temperatures recorded for Stockholm (stippled line) and the Central England (solid line without symbols).

5 **Table captions:**

**Table 1:** Stations with collected sediment core tops and  $\delta^{18}\text{O}$  analyzed on living (rose Bengal stained) *Cassidulina laevigata*.

**Table 2.** AMS  $^{14}\text{C}$  dates obtained for the gravity core 9004 and calibrated calendar ages. All dates presented in Filipsson and Nordberg (2010) and Polovodova Asteman et al. (2013) were re-calibrated using Calib 7.10 (Stuiver *et al.* 2017), the Marine13 calibration dataset (Reimer et al, 2013), and  $\Delta R = 100 \pm 50$ . Asterisks (\*) show dates not used in the final age model due to age reversals.



Figure 1

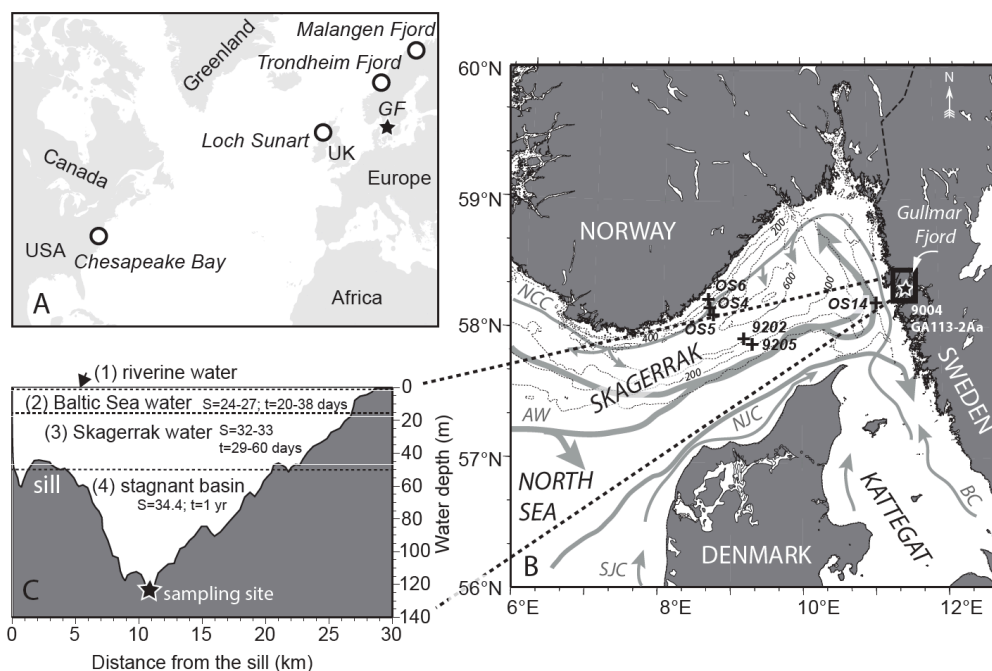




Figure 2

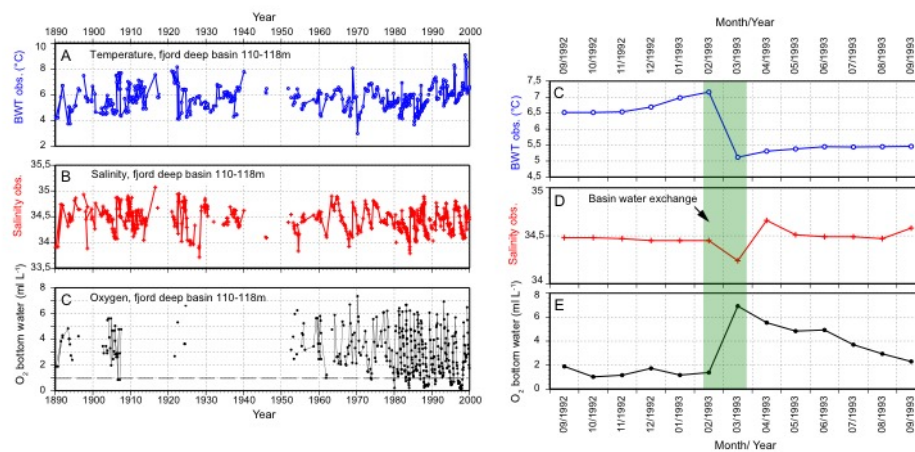




Figure 3

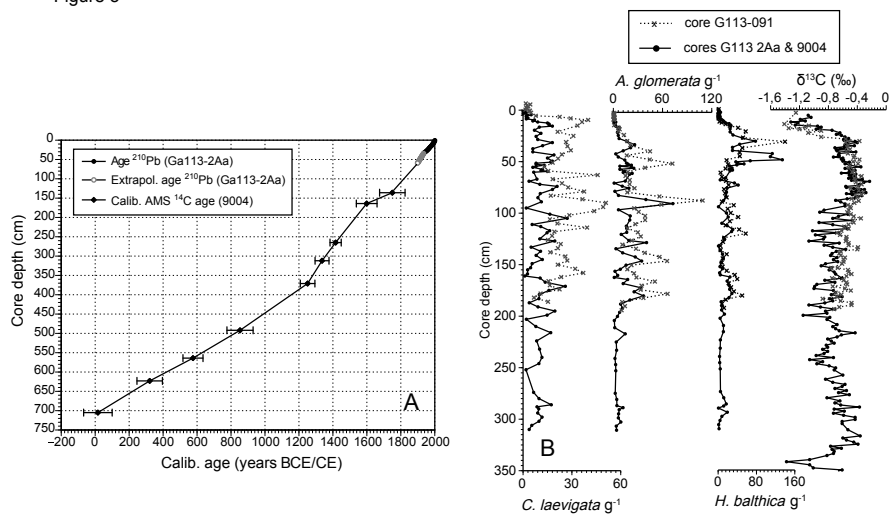




Figure 4

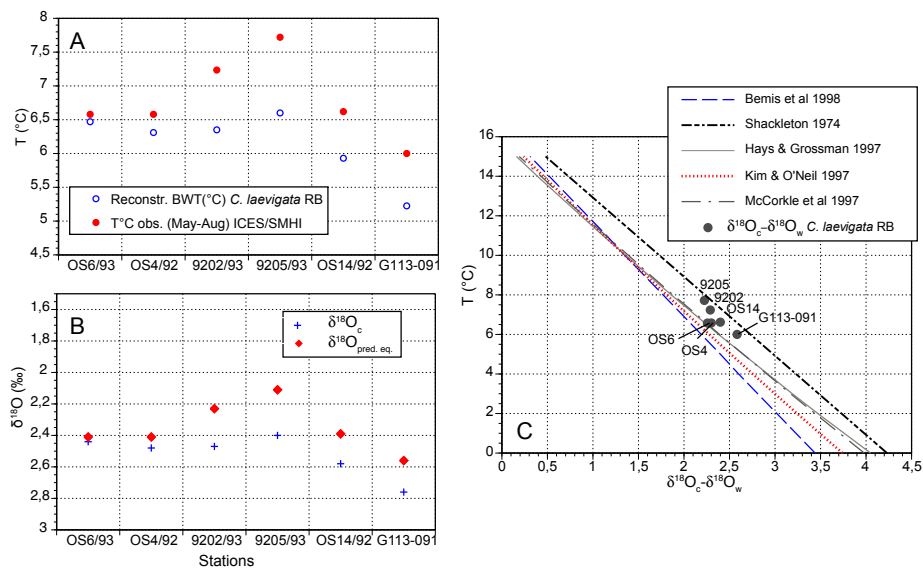




Figure 5

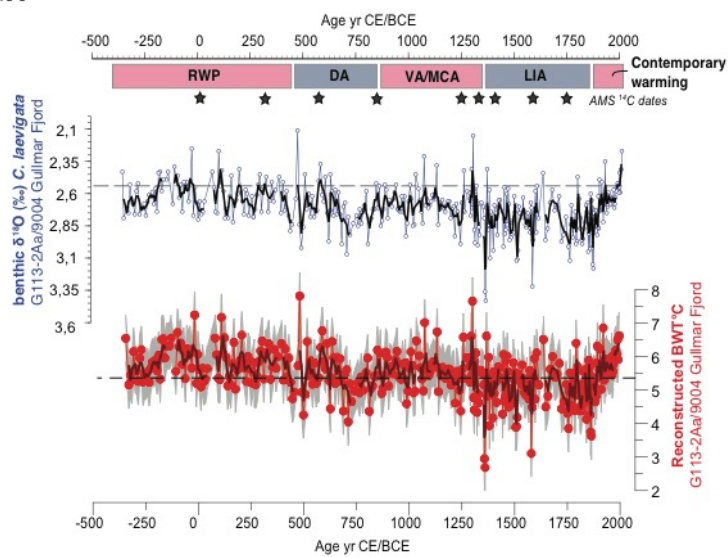




Figure 6

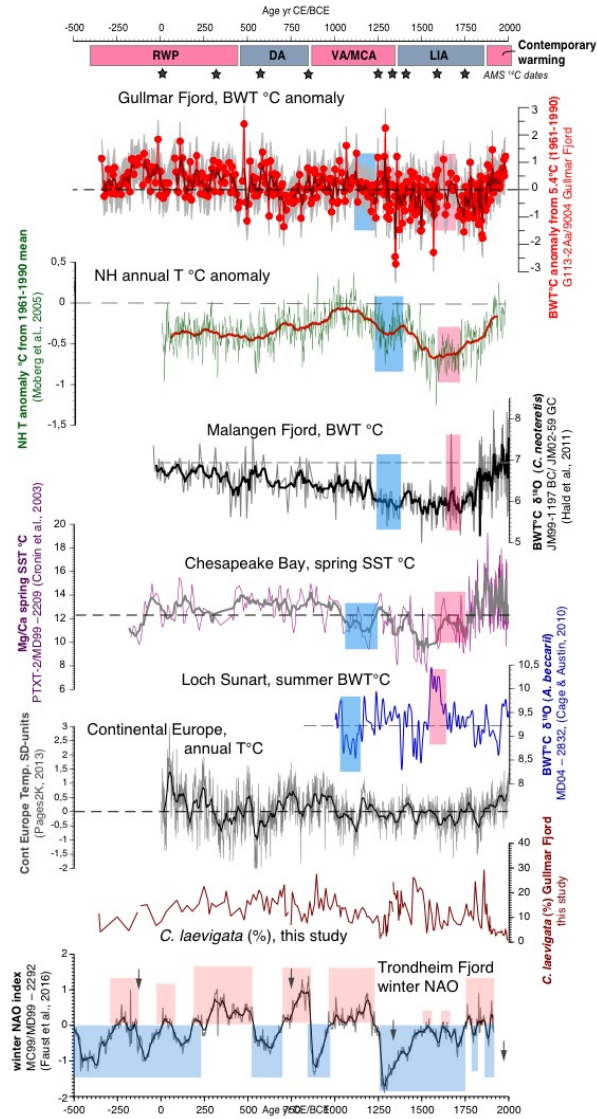




Figure 7

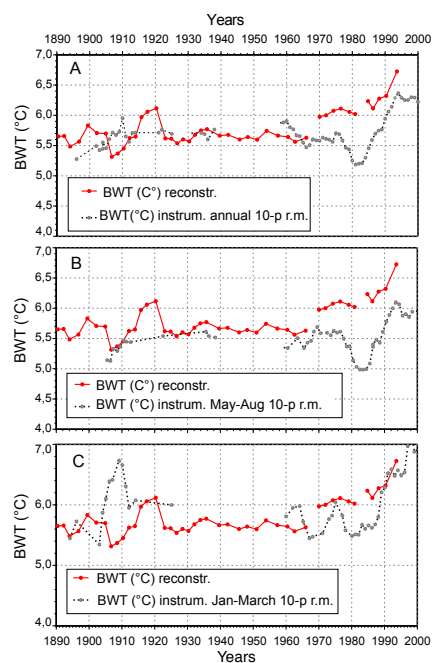
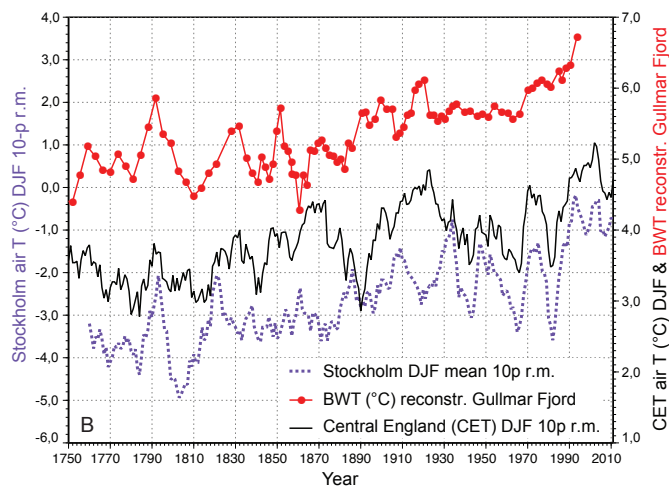




Figure 8





**Table 1:** Stations with collected sediment core tops and  $\delta^{18}\text{O}$  analyzed on living (rose Bengal stained) *Cassidulina laevigata*.

Station	Latitude N	Longitude E	Water depth, m	Sampling date	$\delta^{18}\text{O}$ , ‰
9202	57°56.2'	9°27.3'	177	1992-08-04	2.49
9202	57°56.2'	9°27.3'	177	1992-08-04	2.44
9205	57°58.4'	9°24.0'	294	1992-08-06	2.40
OS14	58°06.06'	10°58.27'	135	1993-05-09	2.58
OS4	58°18.54'	8°54.99'	325	1993-05-04	2.48
OS6	58°21.58'	8°51.01'	177	1992-08-04	2.43
G113-091	58°17.570'	11°23.060'	116	2009-09-01	2.76



**Table 2.** AMS  $^{14}\text{C}$  dates obtained for the gravity core 9004 and calibrated calendar ages. All dates presented in Filipsson and Nordberg (2010) and Polovodova Asteman et al. (2013) were re-calibrated using Calib 7.10 (Stuiver *et al.* 2017), the Marine13 calibration dataset (Reimer et al. 2013), and  $\Delta R = 100 \pm 50$ . Asterisks (\*) show dates not used in the final age model due to age reversals.

Core	Core depth (cm)	Lab. ID	Dated bivalve species	$^{14}\text{C}$ age (years BP)	Error ( $\pm$ )	Calibrated age range, $\pm 1\sigma$ , $\Delta R=100\pm 50$ (years CE/BCE)	Relative probability	Calibrated age, median probability (years CE)
9004	98	Ua-24043	<i>Nuculana minuta</i>	710*	35*	1645-1806*	1	1702*
9004	136	Ua-35966	<i>Nuculana pernula</i>	675	25	1675-1813	1	1750
9004	164	Ua-23075	<i>Yoldiella lenticula</i>	800	40	1538-1664	1	1599
9004	265	Ua-35967	<i>Nucula</i> sp.	1025	30	1356-1372/1383-1465	0.106/0.894	1416
9004	312	Ua-35968	<i>Clamys septemradiatus</i>	1145	25	1295-1389	1	1336
9004	313	Ua-23000	<i>Abra nitida</i>	1305*	45*	1138-1276*	1	1195*
9004	371	Ua-35969	<i>Nucula tenuis</i>	1245	25	1208-1303	1	1251
9004	492	Ua-23001	<i>Abra nitida</i>	1640	45	776-938	1	853
9004	564	Ua-23002	<i>Nuculana minuta</i>	1925	40	517-658	1	576
9004	623	Ua-23003	<i>Thyasira flexuosa</i>	2155	45	246-410	1	321
9004	705	Ua-23004	<i>Thyasira flexuosa</i>	2415	45	68 BCE-102 CE	1	16